PROCEEDINGS OF SCIENCE

Entanglement filtering and improved coarse-graining on two dimensional tensor networks including fermions

Ryo Sakai,[a,*] **Muhammad Asaduzzaman,**[a,b] **Simon Catterall,**[a] **Yannick Meurice**[b] **and Goksu Can Toga**[a]

[a] *Department of Physics, Syracuse University, Syracuse, NY 13244, USA*

[b] *Department of Physics and Astronomy, The University of Iowa, Iowa City, Iowa 52242, USA*

E-mail: rsakai@syr.edu, muhammad-asaduzzaman@uiowa.edu, smcatter@syr.edu, yannick-meurice@uiowa.edu, gctoga@syr.edu

Tensor renormalization group (TRG) has attractive features like the absence of sign problems and the accessibility to the thermodynamic limit, and many applications to lattice field theories have been reported so far. However it is known that the TRG has a fictitious fixed point that is called the CDL tensor and that causes less accurate numerical results. There are improved coarse-graining methods that attempt to remove the CDL structure from tensor networks. Such approaches have been shown to be beneficial on two dimensional spin systems. We discuss how to adapt the removal of the CDL structure to tensor networks including fermions, and numerical results that contain some comparisons to the plain TRG, where significant differences are found, will be shown. The detailed discussion of this work is given in ref. [1].

The 39th International Symposium on Lattice Field Theory (Lattice2022),
8-13 August, 2022
Bonn, Germany

*Speaker

PoS(LATTICE2022)034

1. Introduction

The tensor renormalization group (TRG) [2] has been very successfully applied to spin and gauge models in low dimensions [1]. It allows for high precision calculations of quantities including the free energy using very modest resources—see the recent review and references therein ref. [4]. For practical applications, it is necessary to truncate the number of values that the tensor indices take to a maximal number called the bound dimension. The algorithm appears to be convergent when the values of observables, calculated with some desired precision, stabilize after the bound dimension reaches a sufficiently large value. However, as one approaches a critical point, the required bond dimension may become very large, and the algorithm becomes less efficient. This has been traced to the fact that the standard TRG procedure can drive the coarsened tensor network to an artificial fixed point that is referred to as the corner double line (CDL) tensor [5] [2]. To maintain a proper renormalization group flow improved algorithms have been developed, such as the tensor network renormalization (TNR) [7], the loop-TNR [8], and the gilt-TNR [9] algorithm. In such algorithms, entanglement filtering methods and further optimization steps are incorporated into the network coarsening procedure to eliminate the CDL fixed point.

2. Tensor network representation for Wilson–Majorana fermions

An equivalence between the Ising model and a lattice action for Wilson–Majorana fermions has been shown for two dimensional honeycomb and square lattices [10]. Here we show a tensor network representation of the Wilson–Majorana partition function on a square lattice. While the equivalence has been shown for several choices of boundary conditions, throughout this paper, we assume the periodic and antiperiodic boundary conditions for the spatial and temporal directions, respectively.

The action of the Wilson–Majorana fermion model is given by

$$\begin{aligned} S =& \frac{1}{2}\sum_n \bar{\eta}_n \left(m_\eta + \sum_{\mu=1}^{2} \gamma_\mu \partial_\mu^{\mathrm{S}} - \frac{1}{2}\sum_{\mu=1}^{2} \partial_\mu \partial_\mu^* \right) \eta_n + \frac{1}{2}\sum_n \bar{\chi}_n \left(m_\chi + \sum_{\mu=1}^{2} \gamma_\mu \partial_\mu^{\mathrm{S}} - \frac{1}{2}\sum_{\mu=1}^{2} \partial_\mu \partial_\mu^* \right) \chi_n \\ &+ \sum_n \bar{\eta}_n \left(\gamma_1 \partial_1^{\mathrm{S}} - \gamma_2 \partial_2^{\mathrm{S}} - \frac{1}{2}\partial_1 \partial_1^* + \frac{1}{2}\partial_2 \partial_2^* \right) \chi_n \end{aligned} \tag{1}$$

with two component Majorana spinors $\eta \equiv (\eta_1, \eta_2)^{\mathrm{T}}$ and $\chi \equiv (\chi_1, \chi_2)^{\mathrm{T}}$. The forward, the backward, and the symmetric difference operators are defined by ∂, ∂^*, and $\partial^{\mathrm{S}} = (\partial + \partial^*)/2$, respectively. The masses of the fermions are functions of the reverse temperature κ:

$$m_\eta = \frac{2}{\kappa}\left(\sqrt{2} - 1 - \kappa\right), \qquad m_\chi = -\frac{2}{\kappa}\left(\sqrt{2} + 1 + \kappa\right). \tag{2}$$

The critical point of the system occurs for vanishing m_η, is given by $\kappa_{\mathrm{c}} = \sqrt{2} - 1$, and corresponds to the critical point of the two dimensional Ising model on a square lattice $\beta_{\mathrm{c}} = \tanh^{-1} \kappa_{\mathrm{c}}$.

[1] The higher order TRG [3] can be used for higher dimensional systems, albeit numerical costs strongly depend on the dimensionality.

[2] The fixed point structure of the higher order TRG is also discussed in ref. [6].

By using a representation of γ matrices given by

$$\gamma_1 = \sigma_1 = \begin{pmatrix} 0 & 1 \\ 1 & 0 \end{pmatrix}, \qquad \gamma_2 = \sigma_3 = \begin{pmatrix} 1 & 0 \\ 0 & -1 \end{pmatrix}, \qquad C = -i\sigma_2 = \begin{pmatrix} 0 & -1 \\ 1 & 0 \end{pmatrix}, \tag{3}$$

the partition function can be expressed as

$$\begin{aligned} Z &= \int \left(\prod_n \mathrm{d}\eta_{n,1} \mathrm{d}\eta_{n,2} \mathrm{d}\chi_{n,1} \mathrm{d}\chi_{n,2} \right) e^{-S} \\ &= \sum_{\{x,t\}} \int \prod_n T_{x_n t_n x_{n-\hat{1}} t_{n-\hat{2}}} G_{n, x_n t_n x_{n-\hat{1}} t_{n-\hat{2}}}, \end{aligned} \tag{4}$$

where the bosonic tensor T, whose elements are numerical values, and the Grassmann valued tensor G are defined by

$$\begin{aligned} T_{ijkl} = \int \mathrm{d}\eta_1 \mathrm{d}\eta_2 \mathrm{d}\chi_1 \mathrm{d}\chi_2 e^{(m_\eta+2)\eta_1\eta_2 + (m_\chi+2)\chi_1\chi_2} (-1)^{i_3+i_4} \\ \cdot \eta_2^{l_4} \chi_2^{l_3} \chi_2^{l_2} \eta_2^{l_1} \tilde{\eta}_2^{k_4} \tilde{\chi}_2^{k_3} \tilde{\chi}_2^{k_2} \tilde{\eta}_2^{k_1} \chi_1^{j_4} \eta_1^{j_3} \chi_1^{j_2} \eta_1^{j_1} \tilde{\chi}_1^{i_4} \tilde{\eta}_1^{i_3} \tilde{\chi}_1^{i_2} \tilde{\eta}_1^{i_1}, \end{aligned} \tag{5}$$

and

$$\begin{aligned} G_{n,ijkl} =& \mathrm{d}\alpha_{n,1}^{i_1} \cdots \mathrm{d}\alpha_{n,4}^{i_4} \mathrm{d}\beta_{n,1}^{j_1} \cdots \mathrm{d}\beta_{n,4}^{j_4} \mathrm{d}\bar{\alpha}_{n,1}^{k_1} \cdots \mathrm{d}\bar{\alpha}_{n,4}^{k_4} \mathrm{d}\bar{\beta}_{n,1}^{l_1} \cdots \mathrm{d}\bar{\beta}_{n,4}^{l_4} \\ & \cdot \left[\prod_{s=1}^{4} \left(\bar{\alpha}_{n+\hat{1},s} \alpha_{n,s} \right)^{i_s} \left(\bar{\beta}_{n+\hat{2},s} \beta_{n,s} \right)^{j_s} \right]. \end{aligned} \tag{6}$$

Note that, with the representation of γ matrices (3), the Majorana condition turns out to be

$$\bar{\eta} = \eta^{\mathrm{T}} C = (\eta_2, -\eta_1) \tag{7}$$

together with the same condition on χ. Also, in eq. (5), linear combinations of the spinor components, *e.g.*

$$\tilde{\eta} = \frac{1}{\sqrt{2}} \begin{pmatrix} \eta_1 + \eta_2 \\ -\eta_1 + \eta_2 \end{pmatrix}, \tag{8}$$

are employed for simplicity.

To evaluate eq. (4) on a large space-time volume, one will need to generalize the usual coarse-graining algorithms to allow for blocking of both bosonic and Grassmann tensors. The first application of the TRG to fermion systems was given in refs. [11, 12], and the applications in the context of lattice quantum field theory were in refs. [13–15].

3. Numerical results

In this section, numerical results that are obtained by the normal Grassmann TRG and by Grassmann versions of the improved coarse-graining methods, the loop-TNR [8] and the gilt-TNR [9], are shown.

To demonstrate the equivalence to the Ising model, fig. 1 shows the specific heat of the Wilson–Majorana fermion system. Here the specific heat is calculated by taking the second numerical derivative of the free energy. One can clearly observe a logarithmic growth of the peak height of the specific heat at the critical point $\kappa_c = \sqrt{2} - 1$. The regions $\kappa < \kappa_c$ and $\kappa > \kappa_c$ correspond to the Z_2 symmetric (high temperature) and the broken (low temperature) phases, respectively.

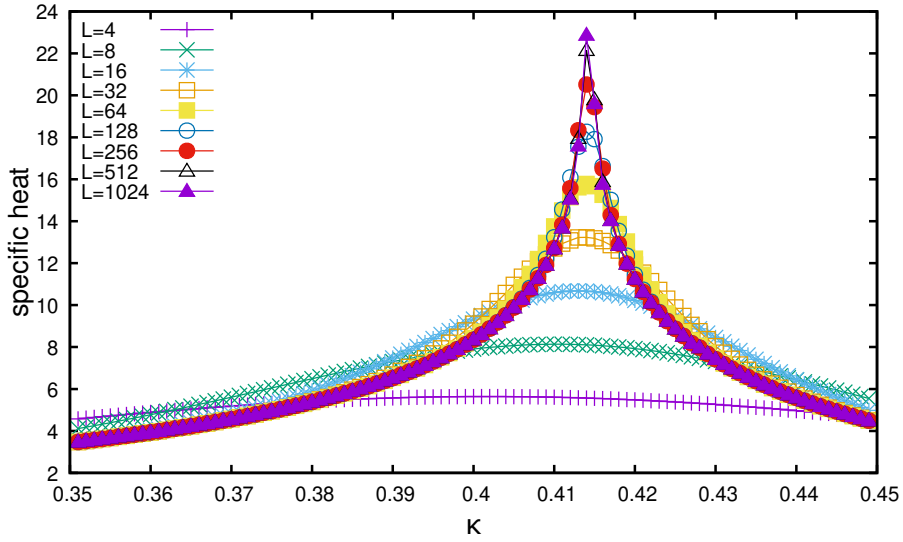

Figure 1: Specific heats of the Wilson–Majorana fermion system.

Figure 2 shows the relative errors of the free energy obtained by the plain Grassmann TRG and the improved ones. The linear system size is set to $L = 1024$ for this comparison. Clearly the Grassmann loop-TNR result shows an exponential improvement of accuracy as compared to the plain Grassmann TRG, and the accuracy reaches better than single precision at a relatively small bond dimension like 10. The Grassmann gilt-TNR shows a similar accuracy to the vanilla Grassmann TRG at lower bond dimensions. At larger bond dimensions, the accuracy of the Grassmann gilt-TNR depends on the hyperparameter ϵ_{gilt} [3]. Optimal ϵ_{gilt} depends on the model, physical parameters, and even on the bond dimension. In our experiments, $\epsilon_{\text{gilt}} = 10^{-6}$ seems like a good choice near the criticality in this model for large bond dimensions.

The renormalization group flow of singular values obtained by the plain Grassmann TRG and the improved algorithms are shown in figs. 3–5. In the figures the singular values are normalized by the largest one at each iteration step, and the horizontal axis is the number of iterations. Notice that the number of iterations i and the number of lattice sites V, which have been compressed to a single tensor, are related by $V = 2^i$ [4]. Clearly the fixed point structure as evidenced by the behavior of the singular values is not reproduced both on and off critical point for the vanilla Grassmann TRG algorithm. This is due to a contamination by short range information that is not properly removed by this algorithm [5]. By contrast, the improved methods show trivial fixed point structures off critical

[3] The hyperparameter ϵ_{gilt} determines how drastically one truncates the entanglement spectra. The detail is discussed in refs. [9, 16].

[4] Note that the number of lattice sites is reduced by $1/2$ through a single iteration step.

[5] On account of the contamination by the short range information, the criticality should shift to a pseudo point when

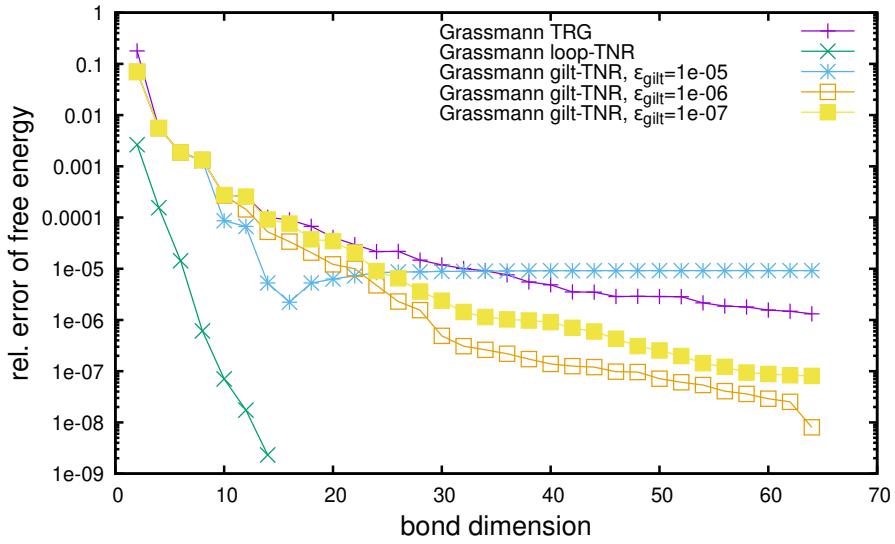

Figure 2: Relative errors of the free energy at the criticality. $L = 1024$.

$\kappa = 0.9999\kappa_c$ and $1.0001\kappa_c$; in the high temperature (symmetric) phase the number of significant singular values is one while in the low temperature (broken) phase there are two degenerate singular values. The fixed point structure is nontrivial only at the criticality, where one can find a scale invariance of the hierarchical structure of the singular values that remains the same against the increasing iteration number. This fact shows that only the improved algorithms are capable of being interpreted as implementing a true renormalization group transformation.

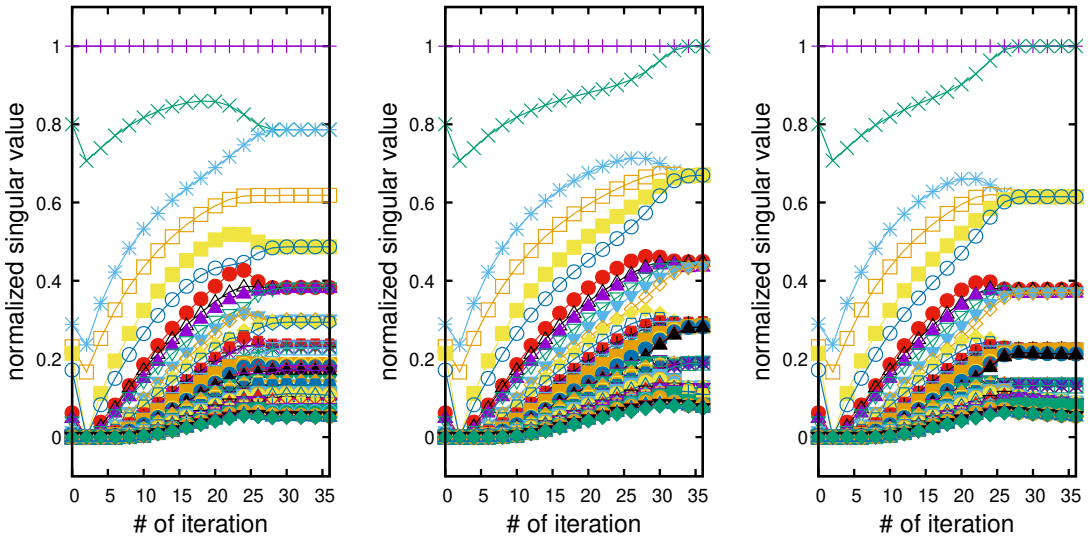

Figure 3: Singular values obtained by Grassmann TRG at $\kappa = 0.9999\kappa_c$ (left), $\kappa = \kappa_c$ (middle), and $\kappa = 1.0001\kappa_c$ (right). The bond dimension is 64.

we use the normal Grassmann TRG.

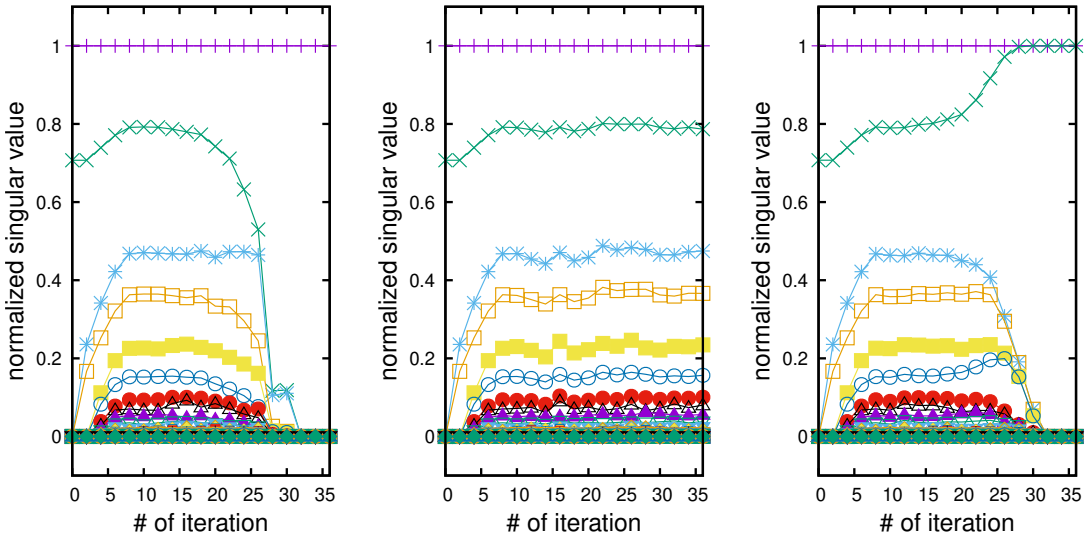

Figure 4: Singular values obtained by Grassmann loop-TNR at $\kappa = 0.9999\kappa_c$ (left), $\kappa = \kappa_c$ (middle), and $\kappa = 1.0001\kappa_c$ (right). The bond dimension is 16.

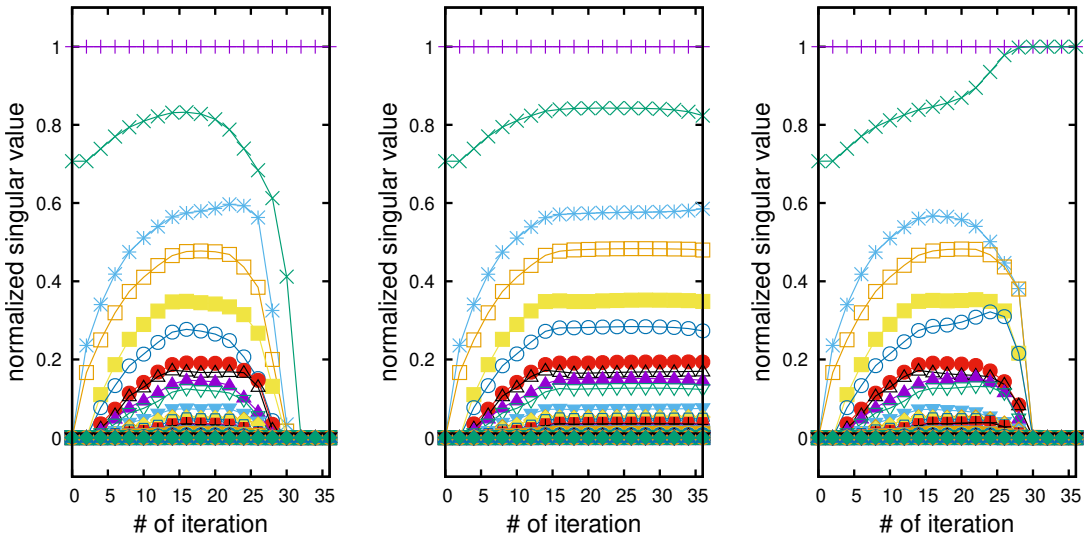

Figure 5: Singular values obtained by Grassmann gilt-TNR at $\kappa = 0.9999\kappa_c$ (left), $\kappa = \kappa_c$ (middle), and $\kappa = 1.0001\kappa_c$ (right). The bond dimension is 64, and $\epsilon_{\text{gilt}} = 10^{-6}$.

4. Conclusion

In this paper, we have shown improved coarse-graining methods adapted to the case of Grassmann valued tensor networks describing fermionic lattice quantum field theories. Both the Grassmann versions of loop-TNR and gilt-TNR show improved accuracy for quantities such as the free energy in comparison to the normal Grassmann TRG. Also, the fixed point structure of the Wilson–Majorana model obtained by the improved algorithms reproduces the known result for the Ising model. (See refs. [7–9] for the analyses on the Ising model.)

Of course, the performance of the improved coarse-graining methods depend on the details of the model. Thus another interesting target would be the staggered Thirring model which was studied using fermion bag methods in ref. [17] [6]. This model has a critical phase and is similar to the classical XY model. Such cases have large numbers of internal d.o.f. and will show more complicated fixed point structure. Indeed, precise investigations on the classical XY model have been reported with the use of the loop-TNR [18, 19]. Thus applying the improved methods to the staggered Thirring model would be a legitimate direction to gain some new insights.

Acknowledgments

We thank the members of the QuLAT Collaboration for valuable discussions. This work was supported in part by the U.S. Department of Energy (DOE) under Award Number DE-SC0019139. This research used resources of the Syracuse University HTC Campus Grid and NSF award ACI-1341006 and the National Energy Research Scientific Computing Center (NERSC), a U.S. Department of Energy Office of Science User Facility located at Lawrence Berkeley National Laboratory, operated under Contract No. DE-AC02-05CH11231 using NERSC award HEP-ERCAP0020659.

References

[1] M. Asaduzzaman, S. Catterall, Y. Meurice, R. Sakai and G.C. Toga, *Improved coarse-graining methods on two dimensional tensor networks including fermions*, 2210.03834.

[2] M. Levin and C.P. Nave, *Tensor renormalization group approach to 2D classical lattice models*, *Phys. Rev. Lett.* **99** (2007) 120601 [cond-mat/0611687].

[3] Z.Y. Xie, J. Chen, M.P. Qin, J.W. Zhu, L.P. Yang and T. Xiang, *Coarse-graining renormalization by higher-order singular value decomposition*, *Phys. Rev.* **B86** (2012) 045139 [1201.1144].

[4] Y. Meurice, R. Sakai and J. Unmuth-Yockey, *Tensor lattice field theory for renormalization and quantum computing*, *Rev. Mod. Phys.* **94** (2022) 025005 [2010.06539].

[5] Z.-C. Gu and X.-G. Wen, *Tensor-Entanglement-Filtering Renormalization Approach and Symmetry Protected Topological Order*, *Phys. Rev.* **B80** (2009) 155131 [0903.1069].

[6] H. Ueda, K. Okunishi and T. Nishino, *Doubling of entanglement spectrum in tensor renormalization group*, *Phys. Rev.* **B89** (2014) 075116 [1306.6829].

[7] G. Evenbly and G. Vidal, *Tensor Network Renormalization*, *Phys. Rev. Lett.* **115** (2015) 180405 [1412.0732].

[8] S. Yang, Z.-C. Gu and X.-G. Wen, *Loop optimization for tensor network renormalization*, *Phys. Rev. Lett.* **118** (2017) 110504 [1512.04938].

[6] To check the performance in an interacting system we have also applied the Grassmann loop-TNR to the staggered $N_f = 2$ Gross–Neveu model on a small lattice in ref. [1].

[9] M. Hauru, C. Delcamp and S. Mizera, *Renormalization of tensor networks using graph independent local truncations*, *Phys. Rev.* **B97** (2018) 045111 [1709.07460].

[10] U. Wolff, *Ising model as Wilson–Majorana Fermions*, *Nucl. Phys.* **B955** (2020) 115061 [2003.01579].

[11] Z.-C. Gu, F. Verstraete and X.-G. Wen, *Grassmann tensor network states and its renormalization for strongly correlated fermionic and bosonic states*, 1004.2563.

[12] Z.-C. Gu, *Efficient simulation of Grassmann tensor product states*, *Phys. Rev.* **B88** (2013) 115139 [1109.4470].

[13] Y. Shimizu and Y. Kuramashi, *Grassmann tensor renormalization group approach to one-flavor lattice Schwinger model*, *Phys. Rev.* **D90** (2014) 014508 [1403.0642].

[14] S. Takeda and Y. Yoshimura, *Grassmann tensor renormalization group for the one-flavor lattice Gross–Neveu model with finite chemical potential*, *Prog. Theor. Exp. Phys.* **2015** (2015) 043B01 [1412.7855].

[15] R. Sakai, S. Takeda and Y. Yoshimura, *Higher order tensor renormalization group for relativistic fermion systems*, *Prog. Theor. Exp. Phys.* **2017** (2017) 063B07 [1705.07764].

[16] C. Delcamp and A. Tilloy, *Computing the renormalization group flow of two-dimensional ϕ^4 theory with tensor networks*, *Phys. Rev. Res.* **2** (2020) 033278 [2003.12993].

[17] V. Ayyar, S. Chandrasekharan and J. Rantaharju, *Benchmark results in the 2D lattice Thirring model with a chemical potential*, *Phys. Rev.* **D97** (2018) 054501 [1711.07898].

[18] A. Ueda and M. Oshikawa, *Resolving the Berezinskii–Kosterlitz–Thouless transition in the two-dimensional XY model with tensor-network-based level spectroscopy*, *Phys. Rev.* **B104** (2021) 165132 [2105.11460].

[19] S. Hong and D.-H. Kim, *Tensor network calculation of the logarithmic correction exponent in the XY model*, *J. Phys. Soc. Jpn.* **91** (2022) 084003 [2205.02773].

PoS(LATTICE2022)034